Electrostatically Driven Topological Freezing of Polymer Diffusion at Intermediate Confinements

Di Jia and Murugappan Muthukumar*
Department of Polymer Science and Engineering, University of Massachusetts, Amherst, Massachusetts 01003, USA

(Received 14 August 2020; revised 23 November 2020; accepted 6 January 2021; published 3 February 2021)

Breaking the paradigm that polymers in crowded aqueous media obey Einstein's law of diffusion, we report a localized nondiffusive hierarchical metastable state at intermediate confinements. Combining electrostatic and topological effects, we can tune the propensity of this new universality class in a quasicoacervate gel system consisting of guest polyamino acid chains inside an oppositely charged host hydrogel. Our observations offer strategies for controlled release and retention of macromolecules in aqueous crowded media, while opening a new direction for understanding topologically frustrated dynamics in polymers and other soft matter systems.

DOI: 10.1103/PhysRevLett.126.057802

Imagine long polymer chains trapped inside very crowded environments created by other interpenetrating macromolecules in aqueous electrolyte solutions at room temperature. We expect the chains to wiggle around and their centers of mass to diffuse, consistent with Einstein's law of diffusion at nonzero temperatures. Indeed, diffusion of polymer chains in their solutions, melts, and under confinement in restrictive porous and gel-like media is the well-established law, with the diffusion coefficient D decreasing monotonically as the extent of crowding and confinement increases [1–29]. Here, we report a breakdown of this paradigm. Using electrostatics and topological confinement, chains are elicited into a locked dynamical state at intermediate confinements, where they do not diffuse for practically very long times, but alive with their internal chain dynamics and endowed functional properties. The propensity of the locked state is also tunable with electrostatic screening. In this Letter, we exhibit this phenomenon from experiments on uniformly charged polypeptide chains confined inside an oppositely charged gel with more than 95% water content at room temperature. Realization of such a dynamically frozen state, for polymers such as DNA and intrinsically disordered proteins in crowded Coulomb-soup-like aqueous media, would enable molecular engines to efficiently search their encoded targets (instead of chasing the constantly moving targets) and to manipulate the movement of polymers using external triggers and macromolecular memory [30–45]. Furthermore, the present "quasicoacervate" system, where one component is an immobile scaffold, is significant in the context of membraneless organelles and mimicry of living matter [30,36,38].

Consider a guest macromolecule trapped inside a host gel (Fig. 1). Its movement is governed by its topological correlation due to its chain connectivity and intrachain and guest-host interactions characterized by three length scales: radius of gyration R_g of the guest, mesh size ξ of the host gel, and segment length ℓ (parametrizing local chemical details of polymer). In isolation, $R_g \sim N^{\nu}$, where N is the degree of polymerization and ν is the size exponent. The vast phenomenology secured over the past several decades can be summarized as three major regimes: (1) Ogston regime [6] for $R_g < \xi > \ell$ [Fig. 1(a)], (2) entropic barrier regime [11,14] for $R_g \simeq \xi > \ell$ [Fig. 1(b)], and (3) reptation regime [1,2,5,7] for $R_g \gg \xi \leq \ell$ [Fig. 1(d)]. $D \sim N^{-y}$, where $y = 1$, 2–3, and 2, respectively, in the three regimes [1–4,9,11,16,17] [Fig. 1(e)]. However, in the fourth regime of intermediate confinement, $R_g > \xi \gg \ell$ [Fig. 1(c)], a guest chain is partitioned among multiple free energy traps, which arise from electrostatic complexation and entropic confinement, so that it can move only by *simultaneously* negotiating these traps. This results in a new state of nondiffusive frustrated dynamics at intermediate confinements.

Theory.—In view of the complexity of the problem, we present only a mean field theory and scaling arguments. Let the linear charge density on the hydrogel be σ at salt concentration c_s. Representing the gel as a 3D assembly of spherical chambers of diameter ξ, consider a chain of N segments, partitioned among n_c contiguous chambers with m_i segments in the ith chamber ($1 \leq i \leq n_c$) [Fig. 2(a)]. Ignoring revisits of chain conformations to chambers, the chain has two "tail" conformations ($i = 1$ and $i = n_c$) and $(n_c - 2)$ "tie" conformations for $1 \leq i \leq n_c$. The free energy of tail and tie conformations with m segments confined inside a chamber can be calculated [46] using field theory and Flory's mean field assumption of adding contributions from confinement entropy, excluded volume, and electrostatic interactions, as

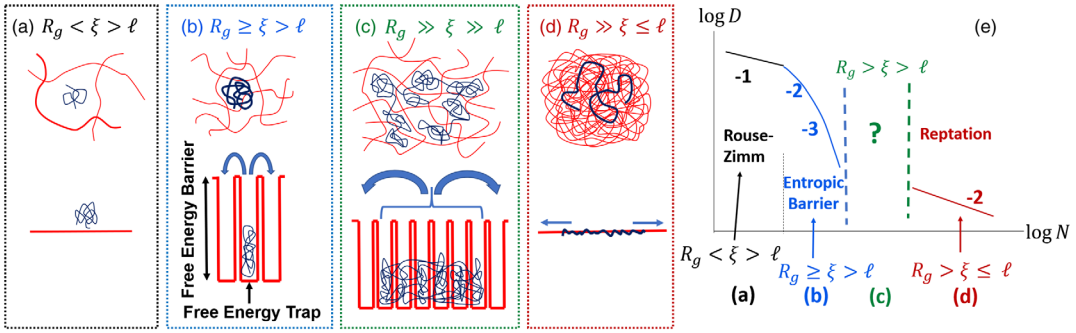

FIG. 1. Dependence of D on N. Nondiffusive frustrated dynamical regime $R_g > \xi \gg \ell$ (c) is flanked by three diffusive regimes corresponding to the Ogston regime (a), entropic barrier regime (b) and reptation regime (d). (e) A summary of the dependence of D on N for all regimes.

$$\frac{F_{\rm tail}(m)}{k_BT} = \ln\left(\frac{\xi}{4\ell}\right) + \frac{2\pi^2}{3}\left(\frac{\ell}{\xi}\right)^2 m + \frac{3}{\pi} v \left(\frac{\ell}{\xi}\right)^3 m^2 - \sigma\xi\left(\frac{\ell_B}{\ell}\right) e^{-\kappa\ell}, \quad (1)$$

$$\frac{F_{\rm tie}(m)}{k_BT} = \ln\left(\frac{\xi^5}{16\pi\ell^5}\right) + \frac{2\pi^2}{3}\left(\frac{\ell}{\xi}\right)^2 m + \frac{3}{\pi} v \left(\frac{\ell}{\xi}\right)^3 m^2 - \sigma\xi\left(\frac{\ell_B}{\ell}\right) e^{-\kappa\ell}, \quad (2)$$

where k_BT is the Boltzmann constant times the temperature. The first two terms on the right-hand side are from confinement entropy, the third term is from excluded volume and electrostatic interactions among guest polymer segments, and the fourth term is from electrostatic attraction between the guest and host. v is the intersegment excluded volume interaction strength, ℓ_B is the Bjerrum length at which intercharge interaction energy is k_BT, and κ is the inverse Debye length $\sim\sqrt{c_s}$. The minimization of free energy of a conformation depicted in Fig. 2(a), $F = F_{\rm tail}(m_1) + \sum_{i=2}^{n_c-1} F_{\rm tie}(m_i) + F_{\rm tail}(m_{n_c})$, with respect to m_i and n_c gives

$$m_i = m_j = \bar{m} = \frac{N}{n_c} \quad \text{and}$$
$$n_c = \sqrt{\frac{3}{\pi}}\left(\frac{\ell}{\xi}\right)^{3/2} \frac{\sqrt{v}N}{\left[\ln\left(\frac{\xi^5}{16\pi\ell^5}\right) - \sigma\xi\frac{\ell_B}{\ell}e^{-\kappa\ell}\right]^{1/2}}. \quad (3)$$

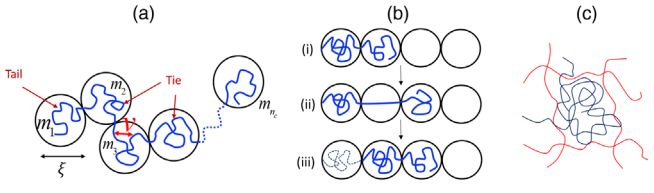

FIG. 2. (a) Partitioning of a chain into meshes. (b) An elementary move to diffuse in the intermediate regime. (c) Complexation between the guest and host hydrogel.

The number of segments m in a particular chamber fluctuates around $\bar{m}$.

We estimate the effective barrier $F^\dagger$ and the disengagement time τ_d (required for a chain to move a distance comparable to its size) as follows. Consider the end chamber with a tail, which jumps into one of the empty neighboring chambers [Fig. 2(b)]. The jump involving $\bar{m}$ ($\gg 1$) monomers can occur in many ways. However, prior experiments [21] show that the jump occurs primarily through a taut conformation (ii) in Fig. 2(b) for the jump from (i) to (iii). We assume in (ii) that guest-host pairs are uncomplexed and the tie chain is taut to length ξ. In addition, for the tail end in state (i) to enter the next chamber, there is a loss of translational entropy of chain end proportional to the volume of the chamber [46]. Using Eqs. (1)–(3), and accounting for the loss of translational entropy of chain end, and with justifiable approximation $v\ell/\xi < 1$, the free energy barrier $F^\dagger = F_{(ii)} - F_{(i)}$ is (see Supplemental Material [47])

$$\frac{F^\dagger}{k_BT} \simeq \ln\left(\frac{1}{96}\frac{\xi^8}{\ell^8}\right) + \sigma\xi\frac{\ell_B}{\ell}e^{-\kappa\ell}, \quad (4)$$

exhibiting the interplay between electrostatic and entropic contributions.

The friction coefficient $\zeta_{\rm chain}$ of the chain to move through $n_c - 1$ such steps, each involving $\bar{m}$ monomers, is

$$\zeta_{\rm chain} = (n_c - 1)\bar{m}\zeta\exp(F^\dagger/k_BT), \quad (5)$$

where ζ is the monomer friction coefficient. Assuming that the chain disengages from its conformation as a one-dimensional random walk (reptation) [1,2,5,7], $(n_c\xi)^2 = 2(k_BT/\zeta_{\rm chain})\tau_d$, where τ_d is the disengagement time. Therefore, τ_d follows from Eqs. (3)–(5) as

$$\tau_d \sim \frac{\zeta}{T} v N^3 \left(\frac{\xi}{\ell}\right)^7 \exp\left[\sigma\xi\frac{\ell_B}{\ell}e^{-\kappa\ell}\right], \quad (6)$$

where logarithmic corrections are suppressed (see Supplemental Material [47]). Since $\xi \gg \ell$, the time

required by the chain to diffuse over its size can become impractically long. Note that the electrostatic complexation elongates the lifetime of the frustrated state.

Therefore, arrest of polymer diffusion into a very long-lived metastable state can occur in the intermediate regime. Nevertheless, since $\xi \gg \ell$, the subchain dynamics inside each mesh is fully allowed. The dynamics of subchains depends on polymer concentration. As is well known [2], dilute solutions with hydrodynamics, semidilute solutions, and concentrated solutions are described by the polymer models of Zimm, Rouse, and reptation, respectively [2,47,55–57]. The fluctuations of the end-to-end distance of the subchain $\mathbf{P}(t) = [\mathbf{R}(m,t) - \mathbf{R}(0,t)]$, proportional to fluctuations in the displacement vector of the host gel, can be measured using dynamic light scattering (DLS) and theory of gel elasticity [58–60]. The scattered intensity correlation from the guest polymer is related to $\langle \mathbf{P}(m,t) \cdot \mathbf{P}(m,0) \rangle$, which is given for $m \gg 1$ by

$$\langle \mathbf{P}(m,t) \cdot \mathbf{P}(m,0) \rangle = \exp\left(-\frac{t}{\tau_0 m^x}\right), \quad x = 3\nu, 2, 3 \qquad \text{(Zimm, Rouse, reptation)}, \tag{7}$$

where ν is the size exponent and τ_0 is the segment relaxation time [2].

Since the numbers of monomers in meshes fluctuate around $\bar{m}$, the dynamics of the localized chain is a superposition of relaxation rates $1/(\tau_0 m^x)$ for each m, resulting in a hierarchy of relaxations. The probability $p(m)$ of having m segments inside a mesh follows from the free energy of confinement F_{conf} given in Eqs. (1) and (2) as [1,46]

$$p(m) \sim \exp(-F_{\text{conf}}/k_B T) \sim e^{\sigma\xi(\frac{\ell_B}{\ell})e^{-\kappa\ell}} \exp(-Bm), \tag{8}$$

where $B = (2\pi^2/3)(\ell/\xi)^2$ denotes the entropic contribution to confinement free energy. The quadratic term in m for F_{conf} is weak due to $v\ell/\xi < 1$; the attractive electrostatic contribution $[-\sigma\xi\ell_B \exp(-\kappa\ell)/\ell]$ is independent of m and appears only to control the propensity of the nondiffusive mode. Thus, $F_{\text{conf}}/k_B T \sim Bm$ ($B \sim \xi^{-2}$ is universal), independent of whether there are electrostatic interactions between the guest and host.

The electric field correlation function $g_1(t)$ measured in DLS is the superposition of Eqs. (7) and (8) (see Supplemental Material [47]),

$$g_1(t) = \langle \mathbf{E}(t) \cdot \mathbf{E}(0) \rangle \sim \int dm p(m) \langle \mathbf{P}(m,t) \cdot \mathbf{P}(m,0) \rangle \sim e^{\sigma\xi(\frac{\ell_B}{\ell})e^{-\kappa\ell}} \int dm e^{-(Bm + \frac{t}{\tau_0 m^x})}. \tag{9}$$

Performing the integral using the saddle point approximation,

$$g_1(t) \sim e^{\sigma\xi(\frac{\ell_B}{\ell})e^{-\kappa\ell}} e^{-(\frac{t}{\tau})^\beta}, \quad \beta = \frac{1}{1+x}, \quad \tau \sim \tau_0 \left(\frac{\xi}{\ell}\right)^{2x}, \tag{10}$$

where β is the stretched exponent, τ is the characteristic time for the hierarchical dynamics, and $x = 3\nu$, 2, and 3 for Zimm, Rouse, and reptation modes, respectively ($\nu = 0.6$ in good solvent and 0.5 for Gaussian chains). The values of β represent hierarchical dynamics of the localized chain at $q\xi \sim 1$, unrelated to the segmental dynamics [2,29,47,55–57], and also unrelated to the dynamics of dense polymer glasses at low temperatures [61]. Simultaneously, the characteristic time τ is stretched far beyond those for segments and subchains, due to the factor $(\xi/\ell)^{2x}$. The amplitude of this frustrated mode increases with lowering c_s ($\kappa \sim \sqrt{c_s}$) as given in Eq. (10).

Experiments.—The two key aspects in designing experiments to elicit the new tunable polymer dynamics are (i) the confinement condition $R_g > \xi \gg \ell$ and (ii) tunability of electrostatics in free energy traps. Cognizant of this, we synthesized a negatively charged gel [poly(acrylamide-co-acrylate gel)] in aqueous solutions containing sodium bromide (NaBr) salt. By judicious control of cross-link density (0.2%), we selected the gel with average mesh size $\xi = 45.2 \pm 3.1$ nm and gel diffusion coefficient $D = (4.78 \pm 0.16) \times 10^{-7}$ cm^2/s (which is related to gel elasticity [59]) in 1.2M NaBr. Oppositely charged poly(L-lysine) (PLL), with its hydrodynamic radius 96 ± 3.2 nm in pregel solution, was chosen as the guest polymer (Supplemental Material [47]). Since the monomer length $\ell \leq 1$ nm, our experimental design satisfies the condition $R_g > \xi \gg \ell$. To avoid irreversible sticking of PLL to the gel, and to tune the guest dynamics in a reasonable range of salt concentration c_s, we chose 10% charge density on the gel. Furthermore, to avoid inhomogeneities inside the gel arising from complexation with the guest, the gel was first synthesized with PLL chains embedded inside at high salt concentration (with no complexation), so that PLL can be uniformly distributed in the host gel. Then, the gel composites were dialyzed for 3 weeks to reach zero-salt limit enabling uniform complexation of PLL with gel. The resultant gel composites were then fully characterized by swelling equilibrium and static and dynamic light scattering. Details of synthesis and characterization are in the Supplemental Material [47]. The key experimental handles are c_s and c_p. We have chosen $c_s = 0$–$1.2M$ to tune the electrostatics and $c_p = 1$, 2, 10, 20, and 100 mg/mL to tune the guest subchain dynamics inside meshes. Also these c_p values correspond to the molar charge ratio (charges on PLL/charged monomers on the gel) $r = 0.1$, 0.2, 1, 2, and 10, respectively, when the charge density of the gel is 10%. All experiments were carried out at 25 °C and neutral pH. The range of scattering wave vector q [$= (4\pi/\lambda)\sin(\theta/2)$, θ is scattering angle, $\lambda = 514.5$ nm], $8.3 \leq q \leq 18.5$ μm^{-1}, used here is

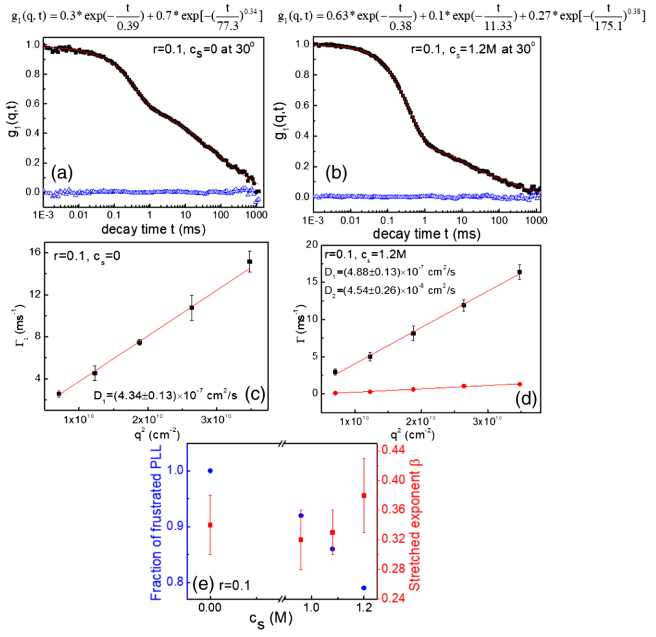

FIG. 3. (a),(b) Normalized field correlation function $g_1(t)$ at scattering angle 30° for $r = 0.1$ and $c_s = 0$ and $1.2M$ (red lines are the best fits and blue triangles are residuals). (c),(d) Corresponding q^2 dependence of relaxation rates Γ. (e) Stretched exponent β and the fraction of frustrated PLL for $r = 0.1$ ($c_p = 1$ mg/mL) at different salt concentrations.

suitable to monitor dynamics of subchains trapped inside meshes of average size 45 nm.

First consider the role of c_s from 0 to $1.2M$, which allows exploration from complete electrostatic dominance to the electrostatics-screened athermal limit (only the residual entropic effect). As examples, the field correlation function $g_1(q, t)$ from DLS at $\theta = 30°$ is given in Figs. 3(a) and 3(b) versus correlation time t for the electrostatic limit $c_s = 0$ and the athermal limit $c_s = 1.2M$, respectively. $g_1(q, t)$ is proportional to PLL concentration correlations and also to displacement correlations of the gel [58,59]. For both cases, the dynamical mode is diffusive if its relaxation rate Γ is proportional to q^2, $\Gamma = Dq^2$, and from the slope of Γ versus q^2, diffusion coefficient D can be obtained. The curve in Fig. 3(a) can be uniquely fitted with two modes: exponential and stretched exponential decays in t, as evident from the red fitting curve to the data and the zero residuals between the fit and raw data. Note the emergence of stretched exponential over three decades in t. Performing the experiment at five different scattering angles, we established that the exponential mode is diffusive where the decay rate $\Gamma_1(q) = D_1 q^2$ [Fig. 3(c)] with $D_1 = (4.34 \pm 0.13) \times 10^{-7}$ cm^2/s. Since this value is close to that for the pure host gel [62,63], D_1 corresponds to gel elasticity. The stretched exponential mode was found as $\exp[-(\Gamma_2 t)^{0.34}]$, where $\Gamma_2 \sim q^0$ (Supplemental Material [47]), associated with nondiffusive hierarchical dynamics of guest PLL. In this salt-free electrostatically controlled condition, there is only one polymer mode that is nondiffusive. The characteristic time $1/\Gamma_2$ for this mode is much longer (~77 ms) than that for the center of mass diffusion ($\tau_N \sim 1$ ms) of guest chain in solutions [2]. Contrary to expectation that oppositely charged guest polymer will permanently stick to the host with $\beta \simeq 0$, the particular design of the system allows dynamical activity at intermediate length scales comparable to ξ, but yet prohibiting center of mass diffusion inside the gel.

On the other hand, for $c_s = 1.2M$, $g_1(q, t)$ [Fig. 3(b)] can be uniquely fitted only by a combination of two exponential decays and one stretched exponential. Measurement of $g_1(q, t)$ at five different scattering angles showed that the two exponential decays are diffusive with diffusion coefficients $D_1 = (4.88 \pm 0.13) \times 10^{-7}$ cm^2/s (similar to D of the gel without PLL) and $D_2 = (4.54 \pm 0.26) \times 10^{-8}$ cm^2/s [Fig. 3(d)], corresponding, respectively, to gel dynamics and diffusion of PLL. The stretched exponential mode is nondiffusive (with rate $\Gamma_3 \sim q^0$) and hierarchical ($\beta = 0.38$). At high c_s with electrostatic screening, the amplitudes of the two guest modes show that the guest dynamics is partitioned into 21% diffusive mode and 79% nondiffusive frustrated dynamical mode (averaged over all scattering angles). The emergence of a pair of diffusional and localized modes at higher c_s from a single localized mode at zero salt signals a pathway to control retention and release of electrostatically captured guest macromolecules inside host media. This effect is shown in Fig. 3(e), where the fraction of frustrated mode decreases monotonically from 100% at $c_s = 0$ to 79% at $c_s = 1.2M$, with the accompanying change in β from 0.34 ± 0.04 to 0.38 ± 0.05. When electrostatic screening releases the guest partially into diffusion, the free energy barriers are progressively reduced, leaving behind only the entropic contribution to the barriers. For the hierarchical dynamics, β shows a transition from electrostatics-driven localization with Rouse subchain dynamics to entropy-driven localization with Zimm subchain dynamics, consistent with theoretical predictions [Eq. (10)] on β and the extent of retention and release.

The role of c_p ($c_p \sim r$) is summarized in Fig. 4 for the two limits $c_s = 0$ and $1.2M$. At $1.2M$ NaBr [Fig. 4(a)], as r increases by increasing c_p, the gel mode (D_1) is insensitive to r if r is low, but is slightly higher at $r = 10$ due to the expected higher guest polymer content inside the matrix. The diffusion coefficient D_2 of PLL continuously decreases with c_p [Fig. 4(b)]. The exponent β for the frustrated guest mode decreases from 0.38 to 0.31, consistent with the expected transition from Zimm to Rouse subchain dynamics. On the other hand, for $c_s = 0$ and $r < 10$, there are only the gel mode (with diffusion coefficient insensitive to r) and the stretched exponential mode. For $r = 10$, where much more guest molecules are present beyond saturation of complexation with the gel, an additional diffusive mode for extra uncomplexed PLL was observed [Fig. 4(c)].

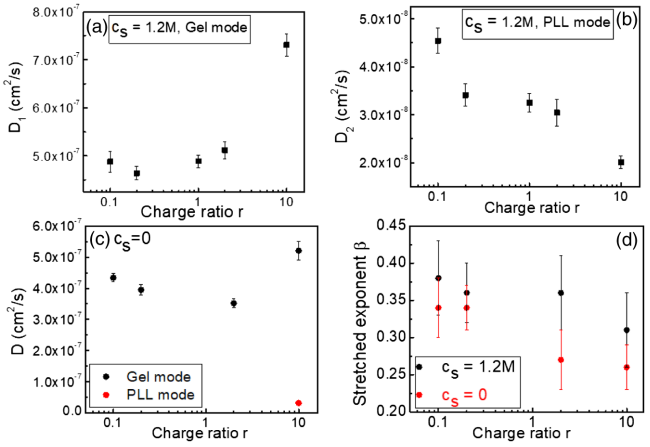

FIG. 4. (a),(b) Diffusion coefficients versus charge ratio r (PLL concentration) in 1.2M NaBr. (a) gel mode and (b) PLL mode. (c) Diffusion coefficients for $c_s = 0$. (d) β versus r for $c_s = 0$ and 1.2M.

In such severely congested situation of strong complexation, extensive interpenetration of guest molecules arises with contributions from entanglements. The experimental value, $\beta = 0.26 \pm 0.03$, is consistent with the prediction of $1/4$ from Eq. (10). As seen in Fig. 4(d), averaged β decreases from 0.34 to 0.26 as charge ratio r increases from 0.1 to 10, showing the transition from Rouse subchain dynamics to reptation subchain dynamics contributing to the frustrated hierarchical dynamics. All experimental findings are consistent with theory.

Summary.—We report a new nondiffusive frustrated dynamics at intermediate confinements in a quasicoacervate system, originating from multiple correlated free energy traps for each chain. Buttressed by theory, we show that the associated hierarchy of chain dynamics is determined by both electrostatics and topological confinements, which can be tuned by electrostatic screening. We observe the hierarchical dynamics to be universal from the strong electrostatics limit to the entropy-dominated athermal limit, with the stretched exponent in a narrow range around $1/3$ at all levels of electrostatic screening. The observed phenomenon, being general for both synthetic and biological contexts, opens new avenues for a fundamental understanding of topologically correlated polymer dynamics in soft matter systems. It also provides new opportunities in designing scaffolds for controlled retention and release of charged macromolecular cargos in crowded aqueous media.

Acknowledgment is made to the National Science Foundation (DMR-2004493) and AFOSR (Grant No. FA9550-20-1-0142) for financial support.

*muthu@polysci.umass.edu

[1] P. G. de Gennes, *Scaling Concepts in Polymer Physics* (Cornell University Press, Ithaca, 1979).
[2] M. Doi and S. F. Edwards, *The Theory of Polymer Dynamics* (Clarendon Press, Oxford, 1986).
[3] P. E. Rouse, J. Chem. Phys. **21**, 1272 (1953).
[4] B. Zimm, J. Chem. Phys. **24**, 269 (1956).
[5] P. G. de Gennes, J. Chem. Phys. **55**, 572 (1971).
[6] A. G. Ogston, B. N. Preston, and J. D. Wells, Proc. R. Soc. A. **333**, 297 (1973).
[7] M. Doi and S. F. Edwards, J. Chem. Soc., Faraday Trans. 2, **74**, 1789 (1978).
[8] O. J. Lumpkin and B. H. Zimm, Biopolymers **21**, 2315 (1982).
[9] H. Kim, T. Chang, J. M. Yhanan, L. Wang, and H. Yu, Macromolecules **19**, 2737 (1986).
[10] M. Rubinstein, Phys. Rev. Lett. **59**, 1946 (1987).
[11] M. Muthukumar and A. Baumgärtner, Macromolecules **22**, 1937 (1989).
[12] D. L. Smisek and D. A. Hoagland, Science **248**, 1221 (1990).
[13] C. R. Calladine, C. M. Collins, H. R. Drew, and M. R. Mott, J. Mol. Biol. **221**, 981 (1991).
[14] M. Muthukumar, J. Non-Cryst. Solids **131–133**, 654 (1991).
[15] E. Arvanitidou and D. A. Hoagland, Phys. Rev. Lett. **67**, 1464 (1991).
[16] N. A. Rotstein and T. P. Lodge, Macromolecules **25**, 1316 (1992).
[17] S. Pajevicl, R. Bansil, and C. Konak, Macromolecules **26**, 305 (1993).
[18] G. W. Slater and S. Y. Wu, Phys. Rev. Lett. **75**, 164 (1995).
[19] J. Rousseau, G. Drouin, and G. W. Slater, Phys. Rev. Lett. **79**, 1945 (1997).
[20] M. Shibayama, Y. Isaka, and Y. Shiwa, Macromolecules **32**, 7086 (1999).
[21] D. Nykypanchuk, H. H. Strey, and D. A. Hoagland, Science **297**, 987 (2002).
[22] P. G. de Gennes, Macromolecules **35**, 3785 (2002).
[23] M. Susoff and W. Oppermann, Macromol. Symp. **291–292**, 212 (2010).
[24] C-C. Lin, E. Parrish, and R. J. Composto, Macromolecules **49**, 5755 (2016).
[25] E. Parrish, M. A. Caporizzo, and R. J. Composto, J. Chem. Phys. **146**, 203318 (2017).
[26] J. Lee, A. Grein-Iankovski, S. Narayanan, and R. L. Leheny, Macromolecules **50**, 406 (2017).
[27] D. Jia and M. Muthukumar, Nat. Commun. **9**, 2248 (2018).
[28] J. Guan, K. Chen, A.-Y. Jee, and S. Granick, J. Chem. Phys. **149**, 163331 (2018).
[29] D. Richter and M. Kruteva, Soft Matter **15**, 7316 (2019).
[30] V. N. Uversky, C. J. Oldfield, and A. K. Dunker, Annu. Rev. Biophys. **37**, 215 (2008).
[31] E. Spruijt, J. Sprakel, M. Lemmers, Martien A. Cohen Stuart, and J. van der Gucht, Phys. Rev. Lett. **105**, 208301 (2010).
[32] E. Spruijt, F. A. M. Leermakers, R. Fokkink, R. Schweins, A. A. van Well, M. A. Cohen Stuart, and J. van der Gucht, Macromolecules **46**, 4596 (2013).
[33] U. Lappan, B. Weisner, and U. Scheler, Macromolecules **49**, 8616 (2016).
[34] J. Li and D. J. Mooney, Nat. Rev. Mater. **1**, 1 (2016).
[35] Y. S. Zhang and A. Khademhosseini, Science **356**, eaaf3627 (2017).

[36] S. F. Banani, H. O. Lee, A. A. Hyman, and M. K. Rosen, Nat. Rev. Mol. Cell Biol. **18**, 285 (2017).
[37] X. Liu, J-P. Chapel, and C. Schatz, Adv. Colloid Interface Sci. **239**, 178 (2017).
[38] A. Borgia, M. B. Borgia, K. Bugge, V. M. Kissling, P. O. Heidarsson, C. B. Fernandes, A. Sottini, A. Soranno, K. J. Buholzer, D. Nettels, B. B. Kragelund, R. B. Best, and B. Schuler, Nature (London) **555**, 61 (2018).
[39] F. G. Hamad, Q. Chen, and R. H. Colby, Macromolecules **51**, 5547 (2018).
[40] M. Yang, J. Shi, and J. B. Schlenoff, Macromolecules **52**, 1930 (2019).
[41] A. H. Slim, R. Poling-Skutvik, and J. C. Conrad, Langmuir **36**, 9153 (2020).
[42] V. M. S. Syed and S. Srivastava, ACS Macro Lett. **9**, 1067 (2020).
[43] S. M. Lalwani, C. I. Eneht, and J. L. Lutkenhaus, Phys. Chem. Chem. Phys. **22**, 24157 (2020).
[44] B. Yu, P. M. Rauscher, N. E. Jackson, A. M. Rumyantsev, and J. J. de Pablo, ACS Macro Lett. **9**, 1318 (2020).
[45] C. E. Sing and S. L. Perry, Soft Matter **16**, 2885 (2020).
[46] M. Muthukumar, Adv. Chem. Phys. **149**, 129 (2012).
[47] See Supplemental Material at http://link.aps.org/supplemental/10.1103/PhysRevLett.126.057802 for more theory and experimental details, which includes Refs. [48–54].
[48] C. C. Han and A. Z. Akcasu, *Scattering and Dynamics of Polymers: Seeking Order in Disordered Systems* (Wiley, New York, 2011).
[49] B. Chu, *Laser Light Scattering: Basic Principles and Practice* (Academic Press, New York, 1991).
[50] D. Jia and M. Muthukumar, J. Am. Chem. Soc. **141**, 5886 (2019).
[51] S. W. Provencher, Comput. Phys. Commun. **27**, 229 (1982).
[52] J. Z. Xue, D. J. Pine, S. T. Milner, X.-I. Wu, and P. M. Chaikin, Phys. Rev. A **46**, 6550 (1992).
[53] S. Morozova and M. Muthukumar, Macromolecules **50**, 2456 (2017).
[54] D. Jia, M. Muthukumar, H. Cheng, C. C. Han, and B. Hammouda, Macromolecules **50**, 7291 (2017).
[55] S. C. Weber, J. A. Theriot, and A. J. Spakowitz, Phys. Rev. E **82**, 011913 (2010).
[56] M. V. Tamm, L. I. Nazarov, A. A. Gavrilov, and A. V. Chertovich, Phys. Rev. Lett. **114**, 178102 (2015).
[57] T. J. Lampo, A. S. Kennard, and A. J. Spakowitz, Biophys. J. **110**, 338 (2016).
[58] K. E. Polovnikov, M. Gherardi, M. Cosentino-Lagomarsino, and M. V. Tamm, Phys. Rev. Lett. **120**, 088101 (2018).
[59] B. J. Berne and R. Pecora, *Dynamic Light Scattering with Applications to Chemistry, Biology, and Physics* (Dover, New York, 1976).
[60] T. Tanaka, L. O. Hocker, and G. B. Benedek, J. Chem. Phys. **59**, 5151 (1973).
[61] G. Nava, M. Rossi, S. Biffi, F. Sciortino, and T. Bellini, Phys. Rev. Lett. **119**, 078002 (2017).
[62] G. B. McKenna and S. L. Simon, Macromolecules **50**, 6333 (2017).
[63] D. Jia and M. Muthukumar, Macromolecules **53**, 90 (2020).